Citation:
O'Kelly B.C., Brinkgreve R.B.J. and Sivakumar V. (2014) Pullout resistance of granular anchors in clay for undrained condition. *Soils and Foundations* Vol. 54, No. 6, pp. 1145–1158. http://dx.doi.org/10.1016/j.sandf.2014.11.009

Pullout resistance of granular anchors in clay for undrained condition

B.C. O'Kelly, R.B.J. Brinkgreve and V. Sivakumar

Brendan C. O'Kelly (corresponding author)
Associate Professor
Department of Civil, Structural and Environmental Engineering,
Museum Building, Trinity College Dublin, Dublin, Ireland.
E-mail: bokelly@tcd.ie Tel. +353 1896 2387 Fax. +353 1677 3072

Ronald B.J. Brinkgreve
Associate Professor
Geo-Engineering Section, Delft University of Technology, The Netherlands
AND
Manager Research and Projects, Plaxis bv, Computerlaan 14, 2628 XK Delft, The Netherlands
E-mail: r.b.j.brinkgreve@tudelft.nl

Vinayagamoothy Sivakumar
Reader in Geotechnical Engineering
SPACE, David Keir Building, Queen's University Belfast, Belfast, UK.
E-mail: v.sivakumar@qub.ac.uk

First submission: 20th January 2013.
Accepted in full: 12th September 2014

Number of Tables: 2
Number of Figures: 13

Abstract:

Granular anchors (GAs) can resist pullout/uplift forces, compression forces and also provide ground improvement. Under pullout loading, a centrally located tendon transmits the applied surface load to the base of the granular column via a base plate attachment, which compresses the column causing significant dilation of the granular material to occur, thereby forming the anchor. This paper describes a program of field testing and numerical modelling of the pullout resistance of GA installations in overconsolidated clay for the undrained (short term) condition. Pertinent modes of failure are identified for different column length to diameter (L/D) ratios. The applied pullout load is resisted in shaft capacity for short GAs or in end-bulging of the granular column for long GAs. In other words, the failure mode is dependent on the column L/D ratio. A novel modification in which the conventional flat base-plate is replaced by a suction cup was shown to significantly improve the undrained ultimate pullout capacity of short GAs.

Keywords: bulging capacity, failure, granular anchor; uplift; ultimate capacity

INTRODUCTION

Granular anchors are a relatively new and promising foundation solution, particularly suited for lightly loaded structures. In addition to the improvement provided to the surrounding ground, granular anchors can resist both pullout/uplift forces and compression forces. Hence they have been adopted, for instance, to prevent foundation uplift caused by flooding (Liu *et al.*, 2006) or to resist foundation heave in expansive clays (Phanikumar *et al*., 2004, 2008; Sharma *et al*., 2004; Srirama Rao *et al*., 2007). Another recent development is the jet mixing anchor pile, a supporting technology particularly suited for foundation pit engineering in soft clay. The ultimate capacity and load–deformation relationship of such piles have been investigated by Xu et al. (2014) using uplift field tests and numerical analyses.

The focus of the present study is to investigate the ultimate capacity and load–deformation relationship of granular anchor (GA) foundations under uplift loading. The GA consists of three main components (Figure 1): a horizontal base plate, a central vertical tendon (metallic rod or stretched cable) and densified granular material introduced into the borehole to form a granular column. Under an applied uplift force (*P*), the tendon transmits the load to the column base via the base plate attachment. The resulting upward pressure over the column base compresses the laterally confined granular column against the sidewall of the soil bore, thereby mobilizing an anchor resistance.

Figure 1. Schematic of granular anchor.

Unlike a conventional concrete anchor cast in-situ, pullout loading can be applied to the GA immediately after its installation. Significant yielding occurs under pullout loading. For short

GAs, this is also accompanied by significant ground heave. In contrast, conventional concrete anchors generally fail by sudden pullout on mobilizing the full shaft capacity, assuming the anchor itself remains structurally sound. The granular column also acts as an effective drainage system to prevent excessive buildup of pore water pressure from occurring (Sivakumar *et al*., 2013).

The success of the GA technique for real applications requires a method to reasonably predict the load–displacement behavior for pullout loading. Various methods of analyses that consider different failure modes, including the vertical slip surface model (friction cylinder method) and block type failures (e.g. inverted cone, circular arc, or in the case of deep anchors, truncated cone), exist for the determination of the ultimate pullout capacity of strip/plate anchors embedded in uniform deposits of sand/clay (Meyerhof and Adams, 1968; Ilamparuthi *et al*., 2002; Merifield *et al*., 2001; Merifield and Sloan, 2006; Khatri and Kumar, 2009, Rangari et al., 2013). Recently, Miyata and Bathurst (2012a, b) investigated the tensile reinforcement load/pullout capacity of steel strips used in reinforced soil walls in Japan. However, the failure modes for GAs are more complex compared with these scenarios; i.e. strip/plate anchors embedded in uniform deposits of sand/clay. This arises on account of the distinctly different response of the densified gravel material (used to construct the granular column) compared with that of the surrounding native material. For the GA, the applied pullout loading at the ground surface is transferred directly to the tendon base-plate assembly and resisted by the granular column. The dilatency of the granular material is a significant factor controlling the GA's pullout capacity. Recent experimental studies by O'Kelly et al. (2013) and Sivakumar et al. (2013), among others, indicate that the applied pullout load is resisted in shaft capacity for short GAs or in localized bulging near the column base for long GAs. In other words, the failure mode depends on the column length to diameter (L/D) ratio.

The motivations for the experimental and numerical studies presented in this paper were to: (a) investigate the operation of GAs, particularly the development of the pullout load–displacement response for the undrained (short term) condition; (b) confirm the postulated modes of failure in shaft capacity or in end bulging and their dependence on the column L/D ratio and ground conditions/properties; (c) develop appropriate methods of analyses for the determination of the ultimate pullout capacity. The research programme involved performing 8 instrumented GA field tests which were subsequently modeled using finite element software. A novel modification of the GA arrangement to improve its undrained ultimate pullout capacity was also modeled numerically.

EXPERIMENTAL PROGRAMME

Ground conditions

Full-scale field trials were performed on 8 GAs installed in the upper Brown Dublin Boulder Clay (BrDBC) layer of the Dublin Boulder Clay (DBC) deposit; an intact lodgement till. This is the primary superficial deposit within the greater Dublin region, Ireland. The DBC deposit is heavily overconsolidated (it was deposited under ice sheets more than 1 km in thickness), with reported overconsolidation ratios of 15–30. The DBC material is significantly stiffer and

O'Kelly B.C., Brinkgreve R.B.J. and Sivakumar V. (2014) Pullout resistance of granular anchors in clay for undrained condition. *Soils and Foundations* Vol. 54, No. 6, pp. 1145–1158.

stronger than other well-characterized tills (e.g. ~ 6–8 times stiffer than typical London Clay and ~ 5 times stiffer than typical Cowden till from the east coast of the UK), at least for the lower strain range (Long and Menkiti, 2007; O'Kelly, 2014). Further details on the geotechnical properties and behavior of the DBC deposit have been reported by Farrell et al. (1995) and Long and Menkiti (2007). The results of interface shear tests on a novel geogrid in DBC backfill material have also been reported by O'Kelly and Naughton (2008).

The BrDBC material is characterized as stiff to very stiff, slightly sandy slightly gravelly silt/clay of low plasticity, with typical liquid limit and plastic limit values of 29% and 16%, respectively (Long and Menkiti, 2007), and a high bulk unit weight of 22 kN/m^3 (Kovacevic et al., 2008). Borehole logs for the test site indicated that the near saturated BrDBC stratum at this location was ~ 1.8 m in depth, with a relatively high stone content (i.e. particle size > 20 mm) of typically 5–15% over this depth. A very clayey/silty gravel layer was encountered in some of the boreholes at a depth of ~ 0.8 m below ground surface level (bgl). The standing groundwater table at the site was located at between 1.8 and 2.0 m bgl.

Figure 2 shows strength against depth data determined for the test area using a 20 t cone penetration test (CPT) rig and unconsolidated–undrained triaxial compression tests. The latter included testing of 'cored' and reconstituted specimens. 'Cored' specimens were obtained from just below the base of the boreholes at final depth using 38 mm diameter sampling tubes. The reconstituted specimens, 100 mm in diameter and 200 mm long, were prepared by standard Proctor-compaction of soil recovered at its in-situ water content using the clay-cutter tool during borehole formation. The CPT undisturbed undrained shear strength was determined as $s_u = (q_c - \sigma_{vo})/N_{kt}$, where: q_c is the cone-tip resistance; σ_{vo} is the overburden pressure and N_{kt} is a cone factor. O'Kelly (2014) reported on CPT testing of the DBC deposit at 3 different sites in the greater Dublin area. From calibrations against measured undrained strengths in triaxial compression, an N_{kt} value of 15 was deemed appropriate for the BrDBC layer and was adopted in the present study. The spiky nature of the CPT trace is explained by the material's high stone content and occasional gravelly layers/lenses, the presence of which were confirmed from the recovered cores. From Figure 2, a general trend of increasing strength with depth is evident, with the remolded undrained shear strength (s_{ur}) at any depth h given by

$$s_{ur} = s_{ur_0} + mh \tag{1}$$

where s_{ur_0} is the remolded undrained strength value corresponding to ground surface level and m is the rate of strength increase with depth [kPa/m]. For the test area, it was determined from Figure 2 that s_{ur_0} = 64 kPa and m = 12.5 kPa/m.

O'Kelly B.C., Brinkgreve R.B.J. and Sivakumar V. (2014) Pullout resistance of granular anchors in clay for undrained condition. *Soils and Foundations* Vol. 54, No. 6, pp. 1145–1158.

Figure 2. Undrained strength against depth determined from CPT cone-tip resistance and triaxial compression tests. Note: data labels identify borehole number – cored (C)/reconstituted (R) triaxial specimen – diameter (mm) – applied cell pressure (kPa).

Anchor installation

The 8 anchors (GA1 to GA8, Table 1) were installed in a line of boreholes formed using a light cable-percussion drilling rig. Boreholes of 150 mm (GA7) and 200 mm (GA3) diameters were formed using clay cutter tools. It was found that in forming holes greater than 0.5 m in depth for the other GA installations, the adhesion/friction generated between the falling cutter tool and sidewalls of the holes was excessive, necessitating the installation of temporary steel casings for these holes. This had the effect of producing slightly larger bores with smooth sidewalls. With the casing removed, the bore diameter was the same as the casing's outer diameter; i.e. 168 and 219 mm for hole diameters of nominally 150 and 200 mm. Into each of these boreholes was placed an M12 threaded rod (i.e. tendon) with a steel base-plate attachment, 148 and 196 mm in diameters for bores of nominally 150 and 200 mm respectively. The base plate was secured at the lower end of the tendon using M12 nuts, one threaded from above the base plate and two threaded from below. The granular columns were constructed by backfilling uniformly graded sub-angular limestone gravel into the boreholes, with compaction to achieve maximum density using the method described by Sivakumar et al. (2013). The grading of the gravel (10 mm nominal particle size) satisfied the minimum recommended ratio between the nominal particle size and column diameter of 1:15.

Table 1. Anchor installation details.

Pullout tests

Pullout forces were applied to the top ends of the anchor tendons using a hydraulic jack supported above the strong cross-beam of a reaction frame. For each GA installation, the load against displacement response of the ground–anchor system was measured using a load cell and a displacement transducer; the latter was mounted on an independent reference beam. The vertical displacement of the ground surface was measured by a second displacement transducer located at a distance of 300 mm from the anchor centerline; i.e. between 190 and 225 mm ($0.87D_o$–$1.5D_o$, where D_o is the installed (initial) column diameter) radially from the sidewalls of the gravel columns for the different GA installations. The displacement response of the ground surface in this region would be an indicator of the anchor's likely failure mechanism, in that significant heave would be expected for block type failures or failure in shaft capacity whereas negligible heave would be expected for GAs failing in end bulging. A single measurement within this zone was deemed sufficient for this purpose. The experimental load–displacement and ground heave response data are modelled in the second part of this study to better understand the GAs performance under pullout loading and associated failure modes. Similar experimental studies performed in the future could consider

O'Kelly B.C., Brinkgreve R.B.J. and Sivakumar V. (2014) Pullout resistance of granular anchors in clay for undrained condition. *Soils and Foundations* Vol. 54, No. 6, pp. 1145–1158.

measuring the ground heave response at two or more radial distances (each a function of the GA's diameter) to provide more experimental data for validation of the modelling. During application of the pullout load, observations were made of the relative vertical movements between the tops of the gravel columns and the surrounding ground surface. The rate of loading was such that the anchor's ultimate pullout capacity was mobilized within a period of 15 min.

EXPERIMENTAL RESULTS

The measured pullout forces and heave of the ground surface at 0.3 m from the anchor centerline are plotted against axial displacement of the anchor tendon (base plate) in Figure 3. Visual observations for anchors GA3 and GA7 having $L \leq 3\,D_o$ (Figure 3(a)) indicated that substantial heave of the surrounding ground occurred on approaching the pullout capacity, with the top surfaces of the gravel columns protruding above the raised ground surface at ultimate pullout capacity. As expected, a larger column length and/or diameter produced greater pullout capacity. For longer columns, the ultimate pullout capacity was generally mobilized for anchor displacements of $\sim D_o/2$; e.g. ~ 85 and ~ 110 mm for GA5 (D_o = 0.168 m) and GA2 (D_o = 0.219 m) respectively. Even though displacements of up to 145 mm were required to mobilize the ultimate pullout capacity of the longest anchors (Figure 3(b)), negligible ground heave (i.e. < 2 mm) was measured at 0.3 m from the anchor centerline. This suggested that these anchors had failed in localized bulging near the base of the gravel columns. This was supported by the observation that at ultimate pullout capacity, the tops of the gravel columns had not moved, remaining level with the surrounding ground surface.

(a) $L/D_o \leq 3$.

(b) $4.4 \leq L/D_o \leq 9.6$.

Figure 3. Experimental values of pullout force and ground heave plotted against axial displacement for granular anchors. Note: (P) and (H), pullout force and heave plots respectively.

EXPERIMENTAL ANALYSES

For conventional concrete/steel tension piles, relative displacements between the anchor and surrounding ground of ~ 0.5% D_o are typically required to mobilize the full shaft capacity. The much larger relative displacements of typically ~ 50% D_o required to mobilize the ultimate pullout capacities of the GAs suggested that there were significant differences between the respective load resistance mechanisms. In particular, one aspect to consider was the significant increase in lateral confinement pressure induced on the granular column during pullout loading on account of the dilation of the dense gravel.

An undrained analysis was justified for the surrounding soil considering: (a) intact BrDBC material has a (horizontal) permeability coefficient value of the order of 10^{-9} m/s (Long and Menkiti, 2007); and (b) the GAs' ultimate capacities were mobilized within 15 min of starting the pullout tests. Note that for the experimental setup described, a vacuum cannot develop in the cavity that forms directly beneath the base plate during pullout on account of the open pore structure of the gravel column

Analogous to the analysis of tension piles, for short GAs failing in shaft capacity, the ultimate pullout load (P_{shaft}) is given by the summation of the shear resistance mobilized over the shaft area and the self-weight of the gravel column (Figure 4(a)):

$$P_{shaft} = \pi D_o L \alpha \overline{s_{ur}} + \frac{\pi D_o^2}{4} L \gamma_g \qquad (2)$$

where α is an adhesion factor; L and D_o are the installed (initial) column length and diameter respectively; $\overline{s_{ur}}$ is the mean remolded undrained strength over the column length and γ_g is the unit weight of gravel forming the granular column.

(a) Failure in shaft capacity (L $<\sim 6\,D_o$, Eq. 2).
(b) Small applied force resisted in shaft resistance over lower section of long column.
(c) Shaft resistance mobilizing upwards along column to resist increasing load.
(d) Failure in localized end bulging of column (L $>\sim 6\,D_o$, Eq. 3).
(e) Encasement of lower section of gravel column to impose failure condition in shaft capacity.
Figure 4. Mobilization of resistance in GAs under pullout loading.

From Eq. (1) and Figure 2, $\overline{s_{ur}}$ = 67–74 kPa for the 8 GAs reported in the present study. As described earlier in the paper, the borehole formation process generally required a temporary steel casing which had the effect of produced a smooth bore sidewall. Under vertical loading, confined compression of the gravel column and dilation of the dense gravel accompanying the large relative displacements between the GA and surrounding soil produced significant increases in the normal stresses acting at the soil–column interface. Under these conditions, some embedment of the gravel particles into the bore sidewall was inevitable. Hence, at ultimate pullout capacity, the rupture surface occurs within the soil next to the column shaft. Significant remolding occurs within this zone on account of the borehole formation process and the large relative displacements occurring between the column shaft and surrounding soil during pullout loading. Under these circumstances, an α value of unity is appropriate, as demonstrated by Sivakumar et al. (2013) from back analysis of the field performance of GAs installed in aged made ground deposits.

For longer GAs, an increasing uplift force applied by the anchor tendon to the base plate is first resisted in shaft resistance over the lower section of the gravel column (Figure 4(b)). The relative movements between the column and surrounding soil mean that the shaft resistance initiates from the column base and develops upwards along the column length. As the applied force increases further, shaft resistance is mobilized over an increasing distance from the column base (Figure 4(c)), up to a point when structural failure of the gravel column occurs by localized end bulging because of a lack of sufficient lateral confinement in the immediate vicinity of the highly stressed column base (Figure 4(d)). With the buildup in end bulging resistance of the column (accompanied by large localized strains), the mobilized shaft resistance reduces back. In other words, the dominant failure mode is governed by the column's L/D_o ratio.

For GAs failing in end bulging, Sivakumar et al. (2013) suggested that the ultimate capacity P_{base} can be determined by adapting the method presented by Hughes et al. (1975) for calculating the ultimate capacity of stone columns under compression (Eq. 3). Localized bulging for stone columns under compression loading and long GAs under pullout loading occurs because of lack of sufficient lateral confinement at the top and bottom ends, respectively, of the granular columns.

$$P_{base} = \frac{\pi D^2 \sigma_{v_{base}}}{4} \tag{3}$$

where D is the diameter of the column bulge; $\sigma_{v_{base}}$ is the bearing pressure at the column base which is estimated by $\sigma_{v_{base}} = \left[\frac{1+\sin\phi'_g}{1-\sin\phi'_g}\right]\left[\sigma_{vc} + N_c^* s_{ur_{base}}\right]$, in which ϕ'_g is the gravel's effective friction angle; N_c^* is a bearing capacity factor considering local shear failure; σ_{vc} is the overburden pressure provided by the surrounding ground and $s_{ur_{base}}$ is the remolded undrained strength in the bulging zone.

The local bearing capacity factor is given by (Gibson and Anderson, 1961):

$$N_c^* = 1 + \log\frac{G_u}{s_{u\,r_{base}}} \tag{4}$$

where G_u is the undrained shear modulus.

The overburden pressure is given by σ_{vc} = $\gamma_s\ L'$, where γ_s is the bulk unit weight of the surrounding soil and L' is the overburden depth to the mid-height of the bulge zone. Sivakumar et al. (2013) suggested that a localized enlargement of approximately 10% in the column diameter occurred on nearing failure in end bulging; i.e. in Eq. (3), $D \approx 1.1\, D_o$. Assuming no significant movement of the gravel material occurs above the bulging zone and conservation of volume for the dense gravel, it can be determined that the predicted length of the bulge zone at pullout failure (typically occurring for axial displacements of ~$D_o/2$) is ~ 2.5 D_o. Hence the mid-height of the bulge zone at ultimate pullout capacity occurs for an overburden depth of $L' \approx L-(D_o+2.5D_o)/2 = L-1.75D_o$ (see Figure 4(d)).

The ultimate pullout load in shaft capacity increases proportionally with, and is strongly sensitive to, the column's L/D ratio. Above a critical aspect ratio $(L/D_o)_{\mathrm{cr}}$, failure in end bulging is the dominant mechanism, with the GA's capacity dependent on $G_u/s_{ur_{base}}$, ϕ'_g and its L/D ratio (see Eq. (3)). As shown later in the paper, for a given column diameter, the ultimate pullout capacity for failure in end bulging increases only marginally with increasing L/D ratio.

Figure 5 shows the experimental ultimate pullout capacity values for the 8 GAs, expressed in the non-dimensional form of P^* (= $4P_{measured}/\pi D_o^2 s_{ur}$), plotted against the columns' L/D ratios. Also included in this figure are envelopes of ultimate resistance in shaft capacity and in end bulging predicted using Eqs. 2 and 3, respectively, but expressed in the form of P^*_{shaft} (= $4L/D_o + L\gamma_g/\overline{s_{ur}}$) and P^*_{base} (= $\sigma_{v_{base}}/s_{ur_{base}}$). An α value of unity (Sivakumar et al., 2013) was used in computing the shaft capacity values. The supposed transition between the different failure modes for the specific ground conditions encountered at the test site occurred for $(L/D_o)_{\mathrm{cr}} \approx 6.2$. The pertinent soil parameter values used in these calculations are listed in Table 2.

Since the GAs had been quickly loaded to failure, with the surrounding soil remaining in an undrained condition, the BrDBC's shear modulus value for computing the local bearing-capacity factor N_c^* in Eq. 4 could be estimated using elastic theory, with an undrained Poisson's ratio (ν_u) value of 0.5. However good-quality undisturbed sampling of the BrDBC layer was not possible on account of its high stone content. Hence, in the present investigation, a single 'operational' G_u value of 3.0 MPa was assumed for the BrDBC layer, and based on the mean $s_{ur_{base}}$ value of ~ 77 kPa determined for the 8 GAs tested, an N_c^* value of 4.7 is obtained using Eq. 4.

Table 2. Material parameter values.

Figure 5. Non-dimensional ultimate pullout capacity against L/D ratio for granular anchors.

Deviations between the experimental and predicted pullout capacity values presented in Figure 5 most likely occurred on account of the inherent variability/strength heterogeneity of the BrDBC layer at the test site. For instance, a very clayey/silty gravel layer had been confirmed from the borehole arisings for a depth of 0.8–0.9 m bgl at the location of anchor GA6. Its presence can also be inferred from the significantly higher CPT cone-tip resistance values mobilized over this depth range (see Figure 2). This would explain why the measured ultimate pullout capacity of GA6 was greater than its shaft capacity predicted using the representative soil property values, reported in Table 2. All four anchors of 200 mm nominal diameter had $L/D \leq 5.5$ (see Table 1), indicating that they had failed in shaft capacity. By contrast, anchors GA5 and GA8 (L/D of 8.7 and 9.6 respectively) failed in end bulging. The hypothesis was substantiated by the insignificant heave (≤ 0.15 mm, Figure 3(b)) of the ground surface measured at 0.3 m from the centerline of these two anchors at ultimate pullout capacity.

NUMERICAL ANALYSES

The numerical analyses were performed using a commercially available finite-element program (PLAXIS 2D 2010 (Brinkgreve et al., 2010)), employing 15 node triangular elements and invoking axisymmetry. The BrDBC material was modeled using a total stress approach (s_u, $\phi_u = 0$), consistent with the experimental conditions. Furthermore, all of the soil parameter values measured were for the undrained condition. The gravel columns were modeled using an effective stress approach. A Mohr–Coulomb model was used for the BrDBC and gravel materials, with consideration of the increase in undrained strength and stiffness with depth. The use of the Mohr–Coulomb model for the BrDBC layer was justified since this material is highly overconsolidated, with reported overconsolidation ratio values ranging 15–30. A typical apparent pre-consolidation (yield) stress value of ~1.0 MPa was estimated from the corrected CPT cone-tip resistance (q_t) data, using the method after Kulhawy and Mayne (1990). This apparent pre-consolidation stress for the test site is in general agreement with the value of 750 kPa for BrDBC determined from in-situ dilatometer tests reported by Lawler et al. (2011).

The Young's modulus values adopted in the numerical analyses required special attention. When using a constant stiffness modulus to represent soil behavior (as in the Mohr–Coulomb model), one should choose a value that is consistent with the stress level and stress path development. The pertinent input parameters are values of undrained (secant) Young's modulus at 50% shear strength corresponding to ground surface level (E_{uo50}) and the rate of increase in this modulus with depth (ΔE_{uo50}). Both values relate to a reference confining pressure of 100 kPa in the triaxial cell since their values tend to increase with confining pressure. Since undisturbed samples were not available, a different approach was adopted in the determination of these stiffness values. Twelve triaxial specimens, each 100 mm in diameter and 200 mm long, were prepared by standard Proctor-compaction of BrDBC material that had been recovered at its natural water content from different depths using the clay cutter tool during borehole formation. These specimens were tested in unconsolidated–

O'Kelly B.C., Brinkgreve R.B.J. and Sivakumar V. (2014) Pullout resistance of granular anchors in clay for undrained condition. *Soils and Foundations* Vol. 54, No. 6, pp. 1145–1158.

undrained triaxial compression, with the stiffness values at 50% shear strength determined from the measured stress–strain curves. The values of E_{uo50} = 7.0 MPa and ΔE_{uo50} = 1.4 MPa/m depth were deduced from regression analysis of the stiffness values at 50% shear strength plotted against depth for the 12 triaxial specimens. It is acknowledged that this approach cannot reproduce the inherent structure of the ground and may result in (significantly) lower values of soil stiffness, especially at small strains. With mean values of L ≈ 1.0 and $s_{u_{r_{base}}}$ ≈ 77 kPa for the 8 GAs tested, these stiffness values indicate G_u ≈ 2.8 MPa (from $G_{\mathrm{u}} = E_{\mathrm{u}}/3$), which is consistent with the value of 3.0 MPa adopted for the BrDBC layer in the experimental analyses. For the drained Poisson's ratio of 0.2 reported for BrDBC (Kovacevic et al., 2008), the E_{uo50} and ΔE_{uo50} values used in the numerical analyses correspond to drained modulus values of 5.6 MPa and 1.1 MPa/m depth respectively.

Considering the very low confinement pressure, a relatively low drained Young's modulus of 4.5 MPa was adopted at ground surface level for the dense gravel column. Its value was considered to increase significantly and proportionately with depth. The ϕ'_g value of 42$^{\mathrm{o}}$ adopted is consistent with reported peak values for dense sub-angular gravel.

The Mohr–Coulomb model applied in PLAXIS 2D (2010) does not allow for dilatency cutoff; i.e. end of dilatency occurs when the soil reaches the critical state. The effect of dilatency angle ψ' was investigated by running simulations with input ψ' values of 10$^{\mathrm{o}}$ and then 5$^{\mathrm{o}}$; i.e. moving towards the critical state ψ' = 0$^{\mathrm{o}}$ value. The interactions between the gravel and BrDBC materials in contact with the top and bottom surfaces, respectively, of the base plate were modeled using an interface friction coefficient value of 0.67.

Long and Menkiti (2006, 2007) and Lawler et al. (2011) reported an average coefficient of earth pressure at-rest (K_0) value of 1.5 for the BrDBC layer, determined from high quality in-situ dilatometer tests. In previous finite element analyses, values of K_0 = 1.5 (Menkiti et al., 2003; Kovacevic et al., 2008) and 3.0 (Lawler et al., 2011) have been adopted for the BrDBC layer. In the absence of data, engineers in Dublin have assumed K_0 values for the BrDBC layer ranging 1.0–1.5 in design (Long and Menkiti, 2007). Based on this evidence, a constant K_0 value of 1.5 with depth was adopted in the present study. For numerical reasons, an undrained Poisson's ratio value of 0.495 was employed along with an apparent cohesion c' value of 0.2 kPa for the gravel.

An axisymmetric model with standard fixities and dimensions of 2.5 m in radius and 2.5 m in depth was used for all of the simulations. This placed the outer vertical boundary at a distance of at least $11\,D_o$ from the sidewall of the gravel column and allowed freedom for any of a number of possibly mechanisms to develop in the BrDBC material, without significant influence from the outer boundary. As for the in-situ condition, the phreatic level was set at 1.8 m bgl.

The calculation scheme was performed in three stages: (a) the initial stresses were generated in the 2.5 m thick BrDBC layer using the K_0 procedure; (b) the GA's gravel column was ‘wished-in-place’; (c) the operation of the anchor during pullout loading (i.e. uniform upward movement of its rigid base plate) was simulated by means of an upward prescribed-displacement condition acting over the base of the gravel column. The horizontal dimension (width) of the prescribed displacement was set equal to that of the base plates used in the field tests, simulating the initial gap of ~ 10 mm present between the outer rim of the base plate and the bore sidewall. A tension cutoff value of 0 kPa was specified throughout the BrDBC layer; i.e. vacuum cannot develop in the cavity that forms directly beneath the base plate during pullout. A number of simulations performed for different mesh densities indicated that coarse meshing (with approximately 1100 elements) was adequate, with pullout failure typically achieved within 5000 steps.

Simulations were also performed for a modified base-plate arrangement that allowed suctions of up to one atmosphere to develop in the cavity formed beneath the base plate during pullout. This condition could occur for (near) saturated, low permeability soils under relatively quick applied loading. Such an anchor arrangement could involve an inverted cup (bucket) attachment at the bottom end of the tendon, which would be driven (embedded) into the base of the borehole (Figure 6(a)). This scenario was modeled by specifying a tension cutoff value of 100 kPa for the BrDBC material. Such an arrangement could also mitigate against the tendency for plastic flow of soil from the bulge zone into the cavity forming at the column base by the upward movement of the anchor (Figure 6(b)).

(a) Proposed installation.
(b) Pullout failure in shaft capacity.
Figure 6. Outline of modified base-plate arrangement for improved GA performance.

NUMERICAL RESULTS

Figure 7 shows predicted GA pullout resistances along with ground heave responses at 0.3 m from the anchor centerlines. Good overall agreement was achieved between the measured and predicted values of ultimate pullout capacity and the corresponding anchor (base plate) displacements. Deviations between the measured and predicted pullout forces arose due to the inherent variability/strength heterogeneity of the BrDBC layer over the test area, with the simulations performed using representative soil parameter values. Another factor was the material model adopted, with the Mohr–Coulomb (linear-elastic perfectly plastic) representation used for the gravel column and surrounding soil predicting a stiffer response for the ground–anchor system and substantially overestimating the ground heave, particularly for experimental GAs having $L/D \le 5.5$ [i.e. < $\left(L/D_o\right)_{\mathrm{cr}}$]. For GA5 and GA8 ($L/D \ge 8.7$), the measured and predicted ground heave responses were in reasonable agreement, significantly smaller in magnitude and approximately increased in proportion with the anchor displacements. Again, the distinctly different ground heave responses for experimental anchors having $L \le 5.5\,D_o$ and $\ge 8.7\,D_o$ indicated different failure mechanisms were at play.

(a) GA7 (L/D = 3.0).

(b) GA2 (L/D = 4.4).

(c) GA1 (L/D = 5.5).

(d) GA8 (L/D = 9.6).

Figure 7. Predictions of pullout resistance and ground heave at 0.3 m from the anchor centerline plotted against anchor displacement, with the plots ordered by increasing column L/D ratio. Unless otherwise stated, simulations are for a constant ψ' = 10°.

Figure 8 shows the extent of the plastic zones predicted in the soil surrounding the GAs at ultimate capacity. From these, the different failure mechanisms occurring predominantly in shaft capacity (Figure 8(a–c)) or in end bulging (Figure 8(d)) can be deduced and are dependent on the column L/D ratio. The enlarged plastic zone formed near the base of anchor GA8 (L/D = 9.6, Figure 8(d)) is indicative of failure in end bulging, consistent with measured and predicted ground heave movements and also with the experimental analyses presented earlier. For all GAs tested having $L \leq 5.5\,D_o$, plastic zones developed over the full column length in the soil next to the soil–column interface (confirmed by contours of displacement plots), indicative of failure in shaft capacity. The extent of the tension zones at the ground surface extended to ~ 1.5 m (~ $7\,D_o$) from the anchor centerline.

(a) GA7 (L/D = 3.0).

(b) GA4 (L/D = 4.6).

(c) GA1 (L/D = 5.5).

(d) GA8 (L/D = 9.6).

Figure 8. Extent of plastic zone predicted at ultimate pullout capacity for a constant ψ' = 10°. Note: Mohr–Coulomb points and tension-cutoff points are indicated by red shading and hollow boxes respectively. Black dotted lines define extents of tension cutoff zones.

Figure 9 shows contours of normal (radial) stress predicted over the column length at ultimate pullout capacity for GA4 and GA8 (L/D of 4.6 and 9.6 respectively). For GA8 (Figure 9(b)), no increase in normal stress was predicted over the upper half of the column length. This can be explained by referring to Figure 4(b–d). Under upward displacement of the base plate caused by increasing pullout load, confined compression of the gravel column and dilation of the dense gravel produces some embedment of the gravel particles into the bore sidewall and a buildup in normal stress that propagates upwards from the column base. The pullout load is resisted in shaft capacity mobilized over this lower section of the column until such point that the normal stresses become too great, resulting in localized end-bulging failure. In this scenario, no increase in normal stress or relative movement (and hence shaft resistance development) occurs over the upper section of the column length. By contrast, for GA4 (Figure 9(b)), the normal stresses increased and relative movements occurred at the interface for the full column length, indicative of full mobilization of the shaft capacity.

O'Kelly B.C., Brinkgreve R.B.J. and Sivakumar V. (2014) Pullout resistance of granular anchors in clay for undrained condition. *Soils and Foundations* Vol. 54, No. 6, pp. 1145–1158.

(a) GA4 (L/D = 4.6).
(b) GA8 (L/D = 9.6).
Figure 9. Predicted normal stress contours (in red color) at ultimate pullout capacity for a constant ψ' = 10^o.

Figure 10 shows the radial expansion of the bore sidewall predicted for different depths (characterized by values of z/D_o, where z is the distance measured from the column base) along the lower section of the gravel column. Figure 10(a, b) shows negligible radial expansion of the gravel columns was predicted for GAs having $L/D \leq 3.0$. Radial strains ε_r (computed as the radial expansion expressed as a percentage of the GA's initial column radius) of less than 2.1% were predicted for the anchor displacements (~ 45 mm, Figure 3(a)) corresponding to the field ultimate pullout capacity. However, for GA5 and GA8 ($L/D \geq 8.7$, Figure 10(g, h)), significant bulging of the columns was predicted over a length of ~ 2–3 D_o from the column base, with ε_r values of ~ 35% predicted for the much larger anchor displacements of at least 100 mm require to mobilize field ultimate pullout capacity (Figure 3(b)). For intermediate L/D values, some radial expansion of the gravel column was also predicted to occur within 2–3 D_o from the column base; e.g. ε_r = 8–14% for the anchor displacements corresponding to the field ultimate pullout capacity of GAs 1, 2 and 4. However this ε_r range is not enough to develop sufficient bulging resistance for failure to occur in end bulging.

Length of the bulge zone

For GAs failing predominantly in end bulging at the test site (i.e. $L/D \geq 6.2$), the predicted bulge length of ~ 2–3 D_o is consistent with the value of ~ 2.5 D_o determined earlier using assumptions reported by Sivakumar et al. (2013) regarding end bulge formation. Some bulging of the gravel columns was also predicted at distances of up to ~ 8 D_o from the column base, although its amount reduced significantly with decreasing depth over this zone.

The ε_r values of ~35% predicted for the anchor displacements corresponding to the field ultimate pullout capacities of GA5 and GA8 were significantly greater than the value of $\varepsilon_r \approx$ 10% postulated by Sivakumar et al. (2013) for failure of the gravel column in end bulging. This is most likely explained by the overestimation of the dilatancy for the gravel in the numerical predictions (which were based on a constant ψ' = 10^o), whereas ψ' = 0^o at critical state. In other words, in the numerical analyses, the ultimate pullout capacity and corresponding ground heave movements for these anchors were overestimated. This is confirmed by comparing Figures 10(g, h) and 11(a, b), with predicted ε_r values reducing by ~ 12% when the input dilatency angle (which remains fixed throughout the numerical simulation) was reduced from 10^o to 5^o.

O'Kelly B.C., Brinkgreve R.B.J. and Sivakumar V. (2014) Pullout resistance of granular anchors in clay for undrained condition. *Soils and Foundations* Vol. 54, No. 6, pp. 1145–1158.

(a) GA3 (L/D = 2.5).
(b) GA7 (L/D = 3.0).
(c) GA2 (L/D = 4.4).
(d) GA4 (L/D = 4.6).
(e) GA6 (L/D = 4.8).
(f) GA1 (L/D = 5.5).
(g) GA5 (L/D = 8.7).
(h) GA8 (L/D = 9.6).

Figure 10. Predicted radial expansion of gravel column for different z/D_o ; where z is the distance from the column base. Unless otherwise stated, simulations are for a constant ψ' = 10^o.

(a) GA5 (L/D = 8.6).
(b) GA8 (L/D = 9.6).

Figure 11. Predicted radial expansion of gravel column for a constant ψ' = 5^o.

Figure 12 shows non-dimensional ultimate pullout capacity ($P*$) predictions for the 8 GAs plotted against column L/D ratio. The predicted $P*$ values for GAs failing in shaft capacity (i.e. L/D < 6.2) were in good agreement with the trend line given by Eq. 2, but expressed in non-dimensional form. However, for anchors GA5 and GA8 failing in end bulging ($L/D \geq$ 8.7), the predicted bulging capacities overestimated the bulge trend line given by Eq. 3, expressed in non-dimensional form. This can be explained by the constant ψ' value of 10^o used in these numerical simulations. Since the dilatency angle is not explicitly considered in Eq. 3, the agreement between the experimental data and the bulge trend line was good (Figure 5). In practice, however, with large localized deformations occurring during column end-bulging, the ψ' value for the gravel reduces towards the critical state ψ' = 0^o value. In order to validate this hypothesis, a number of the simulations were repeated using a lower (constant) ψ' value of 5^o (e.g. see Figure 7(c, d)), which was found to produce much better agreement with the Eq. 3 trend line (see Figure 12).

Figure 12. $P*$ predictions against column L/D ratio.

Modified anchor base-plate for improved pullout capacity

Figure 12 demonstrates the effect of developing suction of one atmosphere in the cavity that forms directly beneath the base plate during pullout loading (see 'With suction cup' data in figure). The predicted improvement in ultimate pullout capacity was found to decay exponentially with the column L/D ratio (Figure 13). From the numerical analyses, the

O'Kelly B.C., Brinkgreve R.B.J. and Sivakumar V. (2014) Pullout resistance of granular anchors in clay for undrained condition. *Soils and Foundations* Vol. 54, No. 6, pp. 1145–1158.

proposed modification of the base-plate arrangement produced significant increases in the undrained ultimate pullout capacity for short GAs; e.g. between ~ 30% (L = 2.5 D_o) and 6% (L = 6.2 D_o) for GAs failing in shaft capacity. However the benefit achieved for GAs failing in end bulging was minor, with negligible improvement achieved for $L/D \geq 10$. Further investigations and validation using experimental field trials are necessary to confirm these findings.

Figure 13. Predicted increase in ultimate pullout capacity for suction of one atmosphere developed beneath the anchor base plate (assuming constant $\psi' = 10^{\mathrm{o}}$ for gravel column).

DISCUSSION

Using experimental and numerical means, this paper has confirmed that failure of GAs predominantly occurs in shaft capacity or in end bulging, depending on the column's L/D ratio. Setting $P_{shaft} = P_{base}$ (Eqs. 2 and 3 respectively) and disregarding the small contribution of the column's self-weight component (i.e. second term in Eq. 2), the transition between failure in shaft capacity and in end bulging occurs for

$$\frac{L_{cr}}{D_o} = \frac{D\sigma_{v_{base}}}{4\alpha\, \overline{s}_{ur}} \qquad (5)$$

with $\sigma_{v_{base}}$ and hence L_{cr}/D_o dependent on ϕ'_g, $s_{ur_{base}}$ and G_u. Note that the value of L_{cr}/D_o increases significantly with ϕ'_g, but only marginally with the $G_u/s_{ur_{base}}$ ratio.

For the particular soil conditions at the test site, the transition between the two failure modes occurred for $\left(L/D_o\right)_{\mathrm{cr}} \approx 6.2$. This value is consistent with experimental observations from other full-scale pullout tests reported for GAs by O'Kelly et al. (2013) and Sivakumar et al. (2013). Numerical predictions of the bulge formation, concentrated within a region extending to 2–3 D_o from the column base, are also consistent with assumptions reported by Sivakumar et al. (2013).

Several researchers (e.g. Phani Kumar and Ramachandra Rao (2000) and Sharma *et al*. (2004)) have reported that end bulging failure of long GAs can be contained by encasing the lower section of the gravel column with geotextile (geofabric tube/sock), thereby providing better performance; i.e. ultimate pullout capacity increases and tendon displacements under pullout loading decrease. The encasement of the lower section of the gravel column would tend to push the zone of bulging higher up the column, where the confining stresses are lower. However, once the column is fully encased for depths greater than ~ 6 D_o, the hoop

O'Kelly B.C., Brinkgreve R.B.J. and Sivakumar V. (2014) Pullout resistance of granular anchors in clay for undrained condition. *Soils and Foundations* Vol. 54, No. 6, pp. 1145–1158.

resistance provided will prevent localized bulging failure from occurring. Hence, under increasing applied pullout loading, the shaft resistance can continue to develop upwards to the top of the gravel column (Figure 4(e)), with failure eventually occurring exclusively in shaft capacity. The numerical analysis has shown that the undrained ultimate pullout capacity can be significantly increased for short GAs installed in (near) saturated, low permeability soils by using an inverted cup (bucket) in place of the conventional flat anchor base plate.

Finally, all of the field tests and numerical simulations presented in this paper relate to the pullout capacity mobilized for the undrained condition. Hence the potential for some softening/swelling of the soil in the vicinity of the column base/bulge zone (e.g. as a result of the groundwater regime or surface water entering down the column shaft) could cause some reduction in the ultimate pullout capacity, particularly for over-consolidated clays.

CONCLUSIONS

Using experimental and numerical means, this paper has confirmed that the undrained ultimate pullout capacity of granular anchors (GAs) is mobilized in shaft capacity or in end bulging, depending on the columns' L/D ratio. During pullout loading, confined compression of the column and dilation of the dense gravel under the large relative displacements occurring at the soil–column interface produce significant increases in the normal stresses and hence some embedment of the gravel particles into the sidewall of the soil bore. For GAs failing in shaft capacity, the rupture surface occurs within the remolded soil next to the column shaft, with the ultimate pullout capacity increasing strongly and proportionally with the column L/D ratio. At the ground surface, the extent of the tension zone in the surrounding soil extends a distance of ~ $7\,D_o$ from the anchor centre line. Above a critical column aspect ratio $\left(L/D_o\right)_{cr}$ value, at ultimate pullout capacity, the column fails structurally by bulging over its lower end (concentrated at ~ 2–3 D_o from the column base), with its capacity dependent on $G_u/s_{ur_{base}}$, ϕ'_g and the column L/D ratio. The field ultimate pullout capacity for end bulging failure was substantially mobilized for anchor displacements of ~ $D_o/2$ and increases only marginally in value with increasing L/D ratio. For the particular ground (intact lodgement till) at the tests site and granular backfill material used to form the columns, the transition between the two failure modes occurred for $\left(L/D_o\right)_{cr} \approx 6.2$. The value of $\left(L/D_o\right)_{cr}$ increases significantly with ϕ'_g and marginally with $G_u/s_{ur_{base}}$. Numerical analyses also showed that the undrained ultimate pullout capacity can be increased (significantly for short GAs) by using an inverted cup/bucket in place of the flat base-plate arrangement used in previous GA setups. The benefit of the proposed modification decayed exponentially with increasing L/D ratio, with no significant gain achieved for $L \geq 10\,D_o$.

Acknowledgements

The authors thank Martin Carney and Eoin Dunne (Department of Civil, Structural and Environmental Engineering, Trinity College Dublin) for assistance in performing the field and laboratory tests presented in this paper. The numerical analyses part of the paper was performed by the lead author at PLAXIS bv, The Netherlands, during a period of sabbatical leave from Trinity College Dublin. This element of the research was performed under the Marie Curie IAPP project NOTES (Grant no. PIAP-GA-2008-230663).

References

Brinkgreve, R.B.J., Swolfs, W.M., and Engin, E. 2010. PLAXIS 2D 2010. PLAXIS bv, The Netherlands.

Farrell, E.R., Coxon, P., Doff, D.H., and Pried'homme, L. 1995. The genesis of the brown boulder clay of Dublin. Quarterly Journal of Engineering Geology, 28(2): 143–152.

Gibson, R.E., and Anderson, W.F. 1961. In-situ measurements of soil properties with the pressuremeter. Civil Engineering and Public Works Review, 56(658): 615–618.

Hughes, J.M.O., Withers, N.J., and Greenwood, D.A. 1975. A field trial of the reinforced effect of a stone column in soil. Géotechnique, 25(1): 31–44.

Ilamparuthi, K., Dickin, E.A., and Muthukrisnaiah, K. 2002. Experimental investigation of the uplift behaviour of circular plate anchors embedded in sand. Canadian Geotechnical Journal, 39(3): 648–664

Khatri, V. N., and Kumar, J. 2009. Vertical uplift resistance of circular plate anchors in clays under undrained condition. Computers and Geotechnics, 36(8): 1352–1369.

Kovacevic, N., Milligan, G.W.E., Menkiti, C.O., Long, M., and Potts, D.M. 2008. Finite element analyses of steep man-made cuts in Dublin boulder clay. Canadian Geotechnical Journal, 45(4): 549–559.

Kulhawy, F.H., and Mayne, P.H. 1990. Manual on Estimating Soil Properties for Foundation Design. Electric Power Research Institute (EPRI), Palo Alto, CA, USA. Report EL-6800.

Lawler, M.L., Farrell, E.R., and Lochaden, A.L.E. 2011. Comparison of the measured and finite element-predicted ground deformations of a stiff lodgement till. Canadian Geotechnical Journal, 48(1): 98–116.

Liu, K.F., Xie, X.Y., Zhang, J.F., and Zhu, X.R. 2006. Compression/tension load capacity of stone column anchors. Proceeding of the ICE, Geotechnical Engineering, 159(3): 161–165.

Long, M., and Menkiti, C.O. 2007. Geotechnical properties of Dublin Boulder Clay. Géotechnique, 57(7): 595–611.

Long, M., and Menkiti, C.O. 2006. Characterisation and engineering properties of Dublin Boulder clay. In: Proceedings of the Second International Workshop on Characterisation and Engineering Properties of Natural Soils – Natural Soils 2006, Singapore (T.S. Tan, K.K. Phoon, D.W. Hight and S. Leroueil (eds)), Taylor and Francis, London, UK, vol. 3, pp. 2003–2045.

Miyata, Y., and Bathurst, R.J. 2012a. Analysis and calibration of default steel strip pullout models used in Japan. Soils and Foundations, 52(3): 481–497.

Miyata, Y., and Bathurst, R.B. 2012b. Measured and predicted loads in steel strip reinforced c–ϕ soil walls in Japan. Soils and Foundations, 52(1): 1–17.

Menkiti, C.O., Long, M., Kovacevic, N., Edmonds, H.E., Milligan, G.W.E., and Potts, D.M. 2004. Trial excavation for cut and cover tunnel construction in glacial till: a case study from Dublin. In Skempton Memorial Conference: Advances in geotechnical engineering

(R.J. Jardine, D.M. Potts and K.G. Higgins (eds), Thomas Telford, London, UK. vol. 2, pp. 1090–1104.

Merifield, R.S., Sloan, S.W., and Yu, H.S. 2001. Stability of plate anchors in undrained clay. Géotechnique, 51(2): 114–153.

Merifield, R.S., and Sloan, S.W. 2006. The ultimate pullout capacity of anchors in frictional soils. Canadian Geotechnical Journal, 43(8): 852–868.

Meyerhof, G.G., and Adams, J.I. 1968. The ultimate uplift capacity of foundations. Canadian Geotechnical Journal, 5(4): 225–244.

O'Kelly, B.C., and Naughton, P.J. 2008. On the interface shear resistance of a novel geogrid with in-plane drainage capability. Geotextiles and Geomembranes, 26(4): 357–362.

O’Kelly, B.C., Sivakumar, V., and Brinkgreve, R.B.J., 2013. Uplift resistance of granular anchors in clay under undrained condition. In: Proceedings of the 1st Workshop on Soil-Structure Interaction organized by the Marie Curie IAPP project NOTES, Trinity College Dublin, Dublin, Ireland. http://www.tara.tcd.ie/handle/2262/66938

O'Kelly, B.C., 2014. CPT testing in Dublin Boulder Clay. In: Proceedings of the Third International Symposium on Cone Penetration Testing (CPT’14), Las Vegas, Nevada, USA, Paper number 2-50, 8 pp. http://www.cpt14.com/cpt14-papers, http://www.tara.tcd.ie/handle/2262/68023

Phani Kumar, B.R., and Ramachandra Rao, N. 2000. Increasing pull-out capacity of granular pile anchors in reactive soils using base geosynthetics. Canadian Geotechnical Journal, 37(4): 870–881.

Phanikumar, B.R., Sharma, R.S., Srirama Rao, A. and Madhav, M.R. 2004. Granular pile anchor foundation (GPAF) system for improving the engineering behaviour of expansive clay beds. Geotechnical Testing Journal, 27(3):1–9.

Phanikumar, B.R., Srirama Rao, A., and Suresh, K. 2008. Field behaviour of granular pile-anchors in reactive soils. Proceedings of the ICE, Ground Improvement, 161(4): 199–206.

Rangari, S.M., Choudhury, D., and Dewaikar, D.M. 2013. Seismic uplift capacity of shallow horizontal strip anchor under oblique load using pseudo-dynamic approach. Soils and Foundations, 53(5): 692–707.

Sharma, R.S., Phanikumar B.R., and Nagendra, G. 2004. Compressive load response of granular piles reinforced with geogrids. Canadian Geotechnical Journal, 41(1): 187–192.

Sivakumar, V., O'Kelly, B.C., Madhav, M.R., Moorhead, C., and Rankin, B. 2013. Granular anchors under vertical loading/axial pull. Canadian Geotechnical Journal, 50(2): 123-132.

Srirama Rao, A., Phanikumar, B.R., Dayakar Babu, R., and Suresh, K. 2007. Pullout behavior of granular pile-anchors in expansive clay beds in situ. Geotechnical and Geoenvironmental Engineering, 133(5): 531–538.

Xu, H.-y., Chen, L.-z., and Deng, J.-l. 2014). Uplift tests of jet mixing anchor pile. Soils and Foundations, 54(2): 168–175.

O’Kelly B.C., Brinkgreve R.B.J. and Sivakumar V. (2014) Pullout resistance of granular anchors in clay for undrained condition. *Soils and Foundations* Vol. 54, No. 6, pp. 1145–1158.

Anchor number	Temporary casing required	Borehole diameter, D_o (m)	Anchor length, L (m)	Anchor aspect ratio, L/D_o	Ultimate field pullout capacity (kN)
GA1	Yes	0.219	1.20	5.5	51.0
GA2	Yes	0.219	0.96	4.4	43.0
GA3	No	0.200	0.50	2.5	19.1
GA4	Yes	0.219	1.00	4.6	47.0
GA5	Yes	0.168	1.47	8.7	42.5
GA6	Yes	0.168	0.80	4.8	33.0
GA7	No	0.150	0.45	3.0	12.8
GA8	Yes	0.168	1.62	9.6	42.0

Table 1. Anchor installation details.

Material	**Value**
Surrounding soil	
Bulk unit weight, γ_s (kN/m^3)	22
Remolded undrained strength at ground surface level, s_{ur0} (kPa)	64
Rate of increase in undrained strength with depth, *m* (kPa/m)	12.5
Undrained Young's modulus at ground surface, E_{uo50} (MPa)	7.0
Rate of increase of Young's modulus with depth, ΔE_{uo50} (MPa/m)	1.4
Undrained Poisson's ratio, υ_u	0.5
Coefficient of earth pressure at rest, K_0	1.5
Gravel column	
Bulk unit weight, γ_g (kN/m^3)	20
Apparent cohesion, c' (kPa)	0.2
Effective friction angle, ϕ'_g (degree)	42
Dilatency angle, ψ' (degree)	10
Drained Young's modulus at ground surface level (MPa)	4.5
Rate of increase in Young's modulus with depth (MPa/m)	30
Drained Poisson's ratio, υ'	0.3

Table 2. Material parameter values.

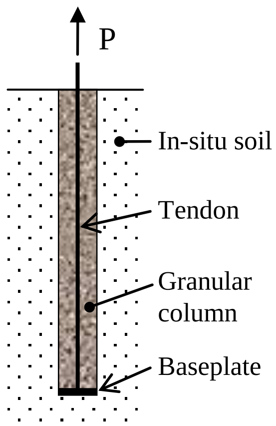

Figure 1. Schematic of granular anchor.

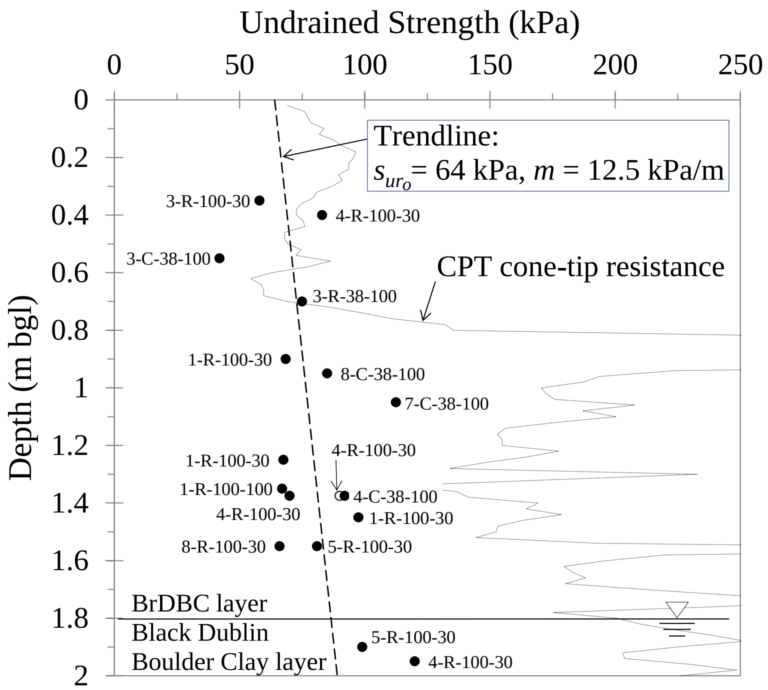

Figure 2. Undrained strength against depth determined from CPT cone-tip resistance and triaxial compression tests. Note: data labels identify borehole number – cored (C)/reconstituted (R) triaxial specimen – diameter (mm) – applied cell pressure (kPa).

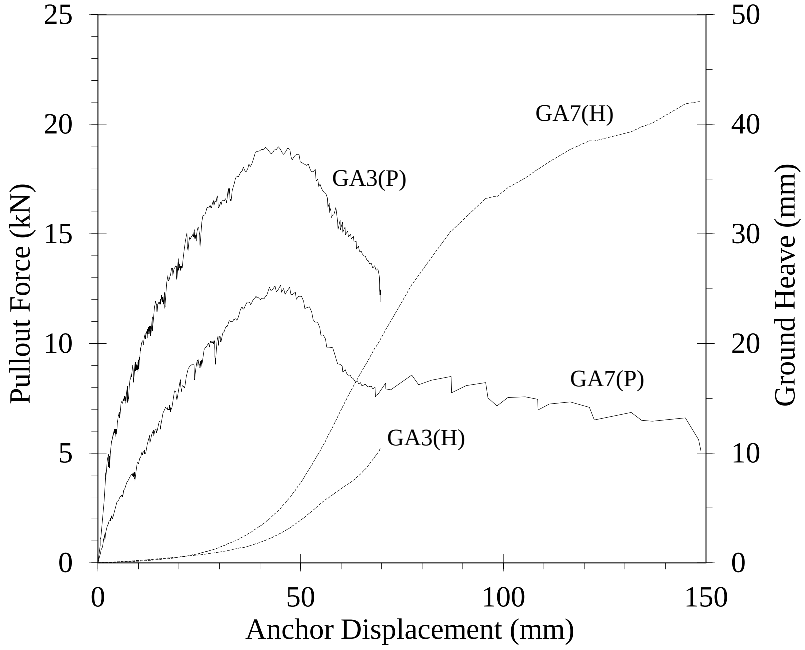

(a) $L/D_o \leq 3$.

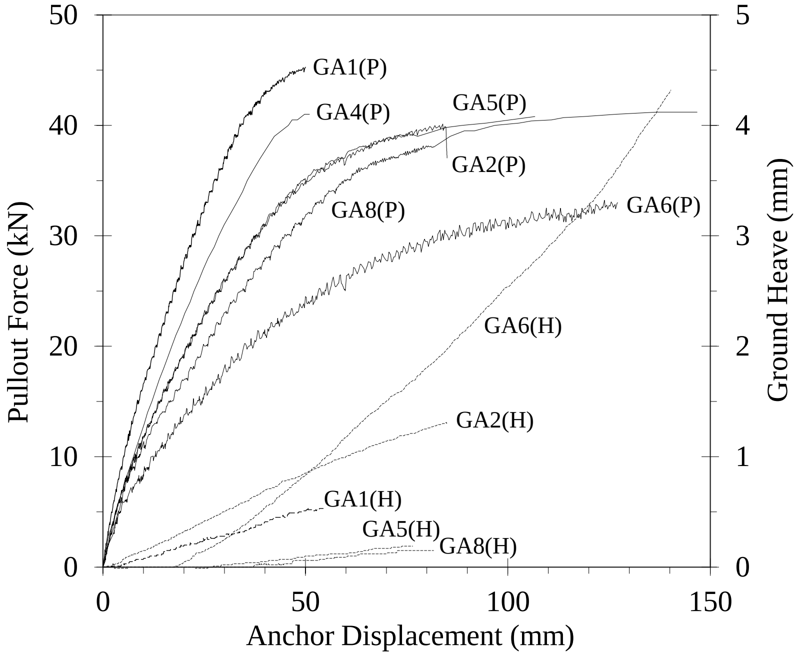

(b) $4.4 \leq L/D_o \leq 9.6$.

Figure 3. Experimental values of pullout force and ground heave plotted against axial displacement for granular anchors. Note: (P) and (H), pullout force and heave plots respectively.

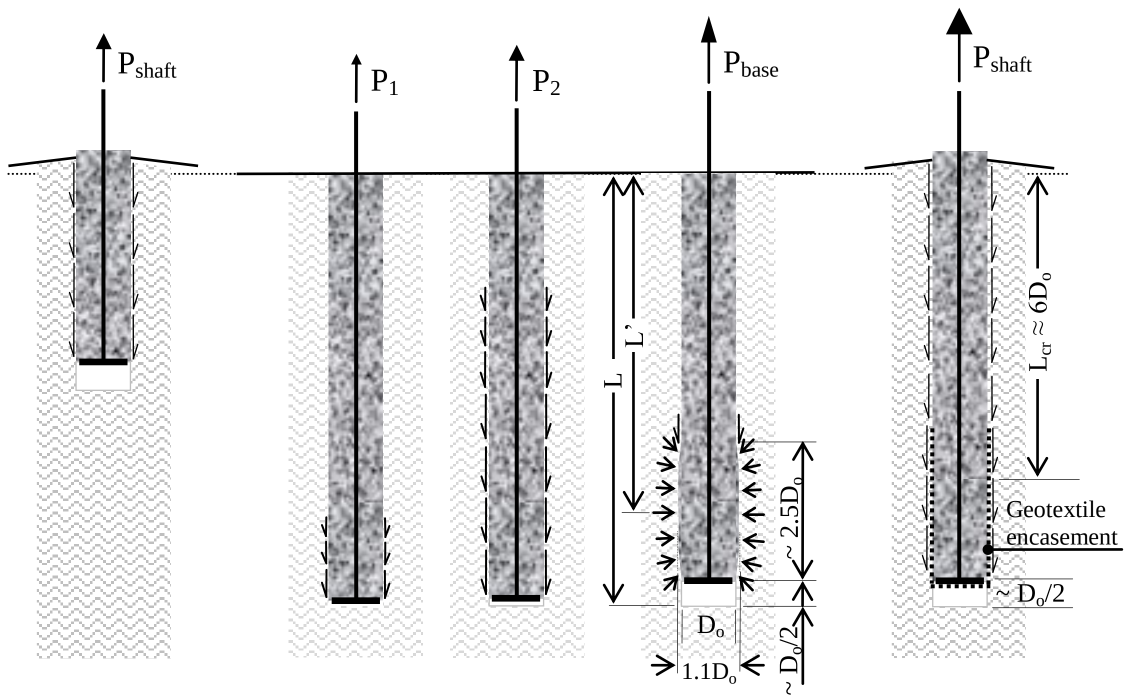

(a) (b) (c) (d) (e)

Figure 4. Mobilization of resistance in GAs under pullout loading: (a) Failure in shaft capacity ($L < \sim 6D_o$, Eq. 2); (b) Small applied force resisted in shaft resistance over lower section of long column; (c) Shaft resistance mobilizing upwards along column to resist increasing load; (d) Failure in localized end bulging of column ($L > \sim 6D_o$, Eq. 3); (e) Encasement of lower section of gravel column to impose failure condition in shaft capacity.

O'Kelly B.C., Brinkgreve R.B.J. and Sivakumar V. (2014) Pullout resistance of granular anchors in clay for undrained condition. *Soils and Foundations* Vol. 54, No. 6, pp. 1145–1158.

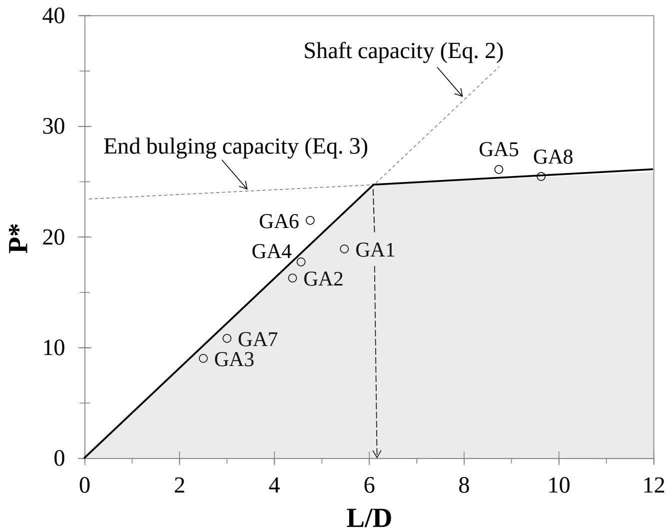

Figure 5. Non-dimensional ultimate pullout capacity against L/D ratio for granular anchors.

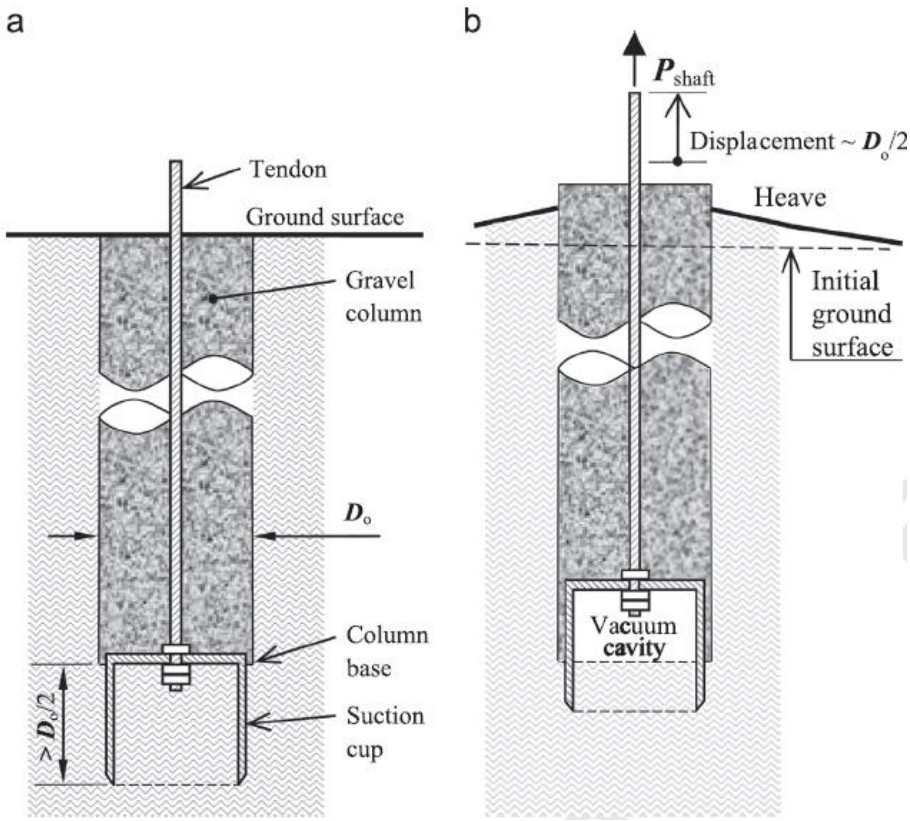

Figure 6. Outline of modified base-plate arrangement for improved GA performance: (a) Proposed installation; (b) Pullout failure in shaft capacity.

O'Kelly B.C., Brinkgreve R.B.J. and Sivakumar V. (2014) Pullout resistance of granular anchors in clay for undrained condition. *Soils and Foundations* Vol. 54, No. 6, pp. 1145–1158.

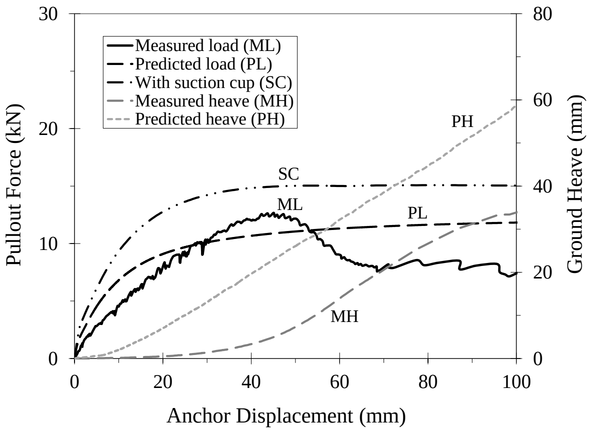

(a) GA7 (L/D = 3.0).

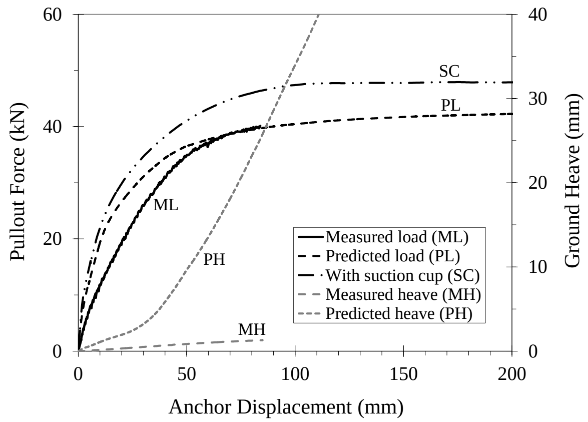

(b) GA2 (L/D = 4.4).

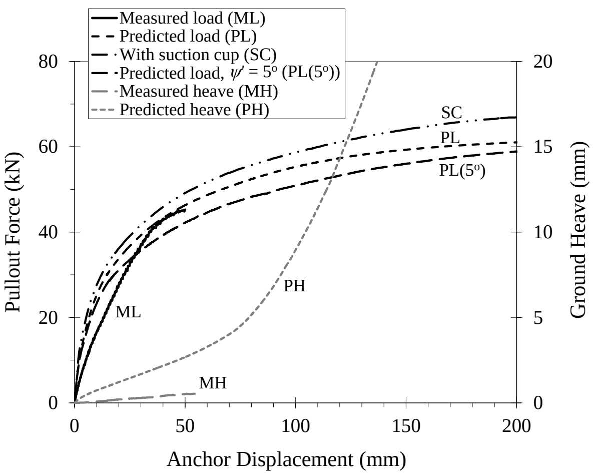

(c) GA1 (L/D = 5.5).

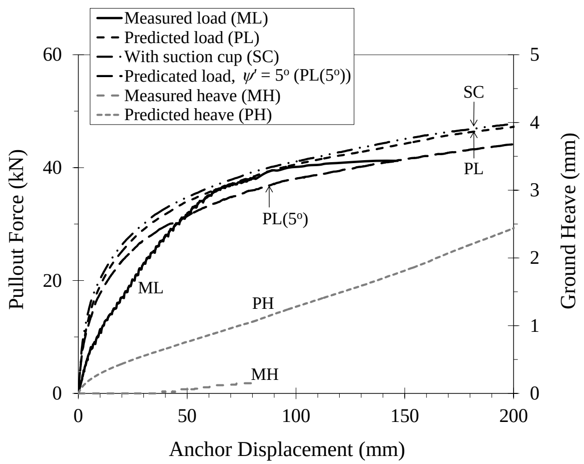

(d) GA8 (L/D = 9.6).

Figure 7. Predictions of pullout resistance and ground heave at 0.3 m from the anchor centerline plotted against anchor displacement, with the plots ordered by increasing column L/D ratio. Unless otherwise stated, simulations are for a constant ψ' = 10°.

O'Kelly B.C., Brinkgreve R.B.J. and Sivakumar V. (2014) Pullout resistance of granular anchors in clay for undrained condition. *Soils and Foundations* Vol. 54, No. 6, pp. 1145–1158.

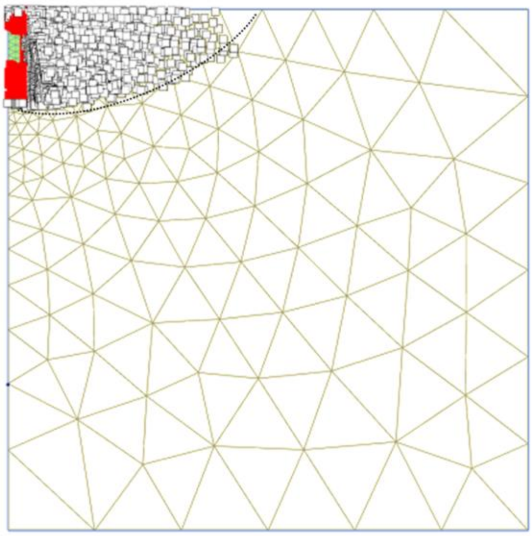

(a) GA7 (L/D = 3.0).

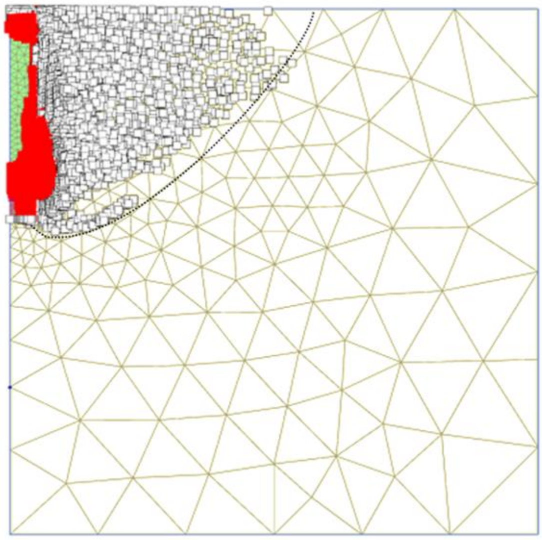

(b) GA4 (L/D = 4.6).

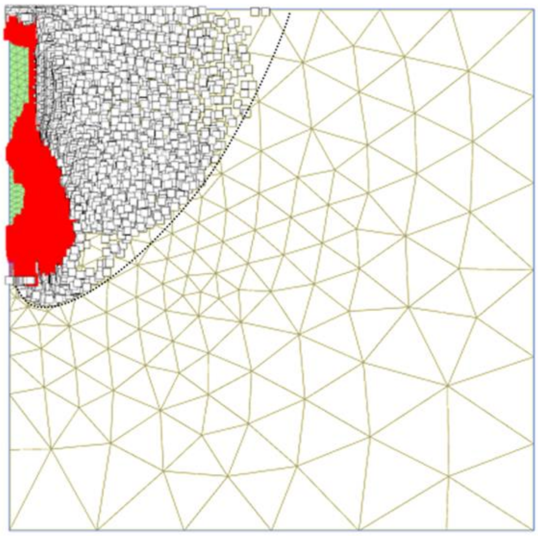

(c) GA1 (L/D = 5.5).

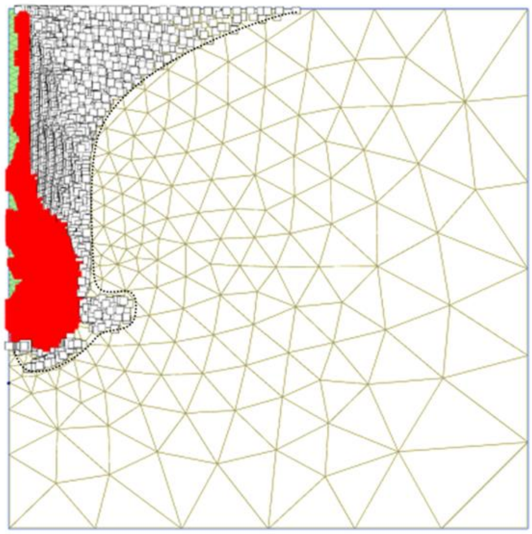

(d) GA8 (L/D = 9.6).

Figure 8. Extent of plastic zone predicted at ultimate pullout capacity for a constant ψ' = 10°. Note: Mohr–Coulomb points and tension-cutoff points are indicated by red shading and hollow boxes respectively. Black dotted lines define extents of tension cutoff zones.

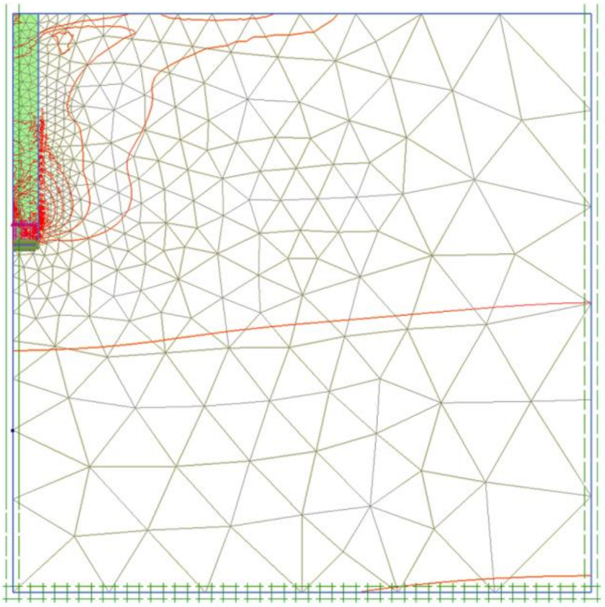

(a) GA4 (L/D = 4.6).

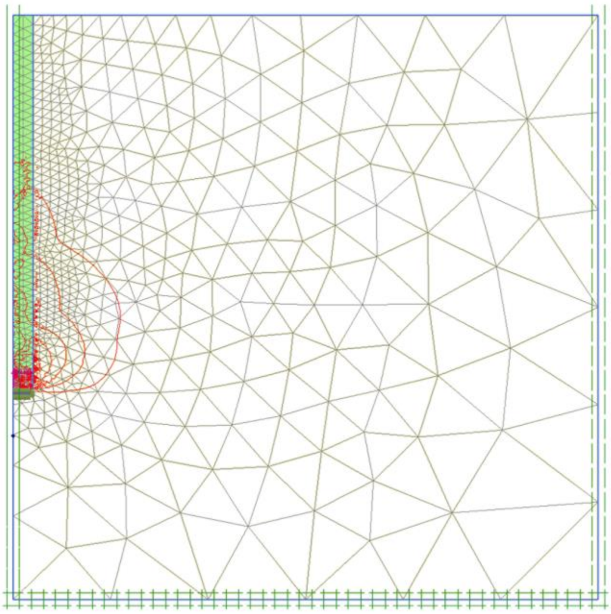

(b) GA8 (L/D = 9.6).

Figure 9. Predicted normal stress contours (in red color) at ultimate pullout capacity for a constant ψ' = 10^{o}.

O'Kelly B.C., Brinkgreve R.B.J. and Sivakumar V. (2014) Pullout resistance of granular anchors in clay for undrained condition. *Soils and Foundations* Vol. 54, No. 6, pp. 1145–1158.

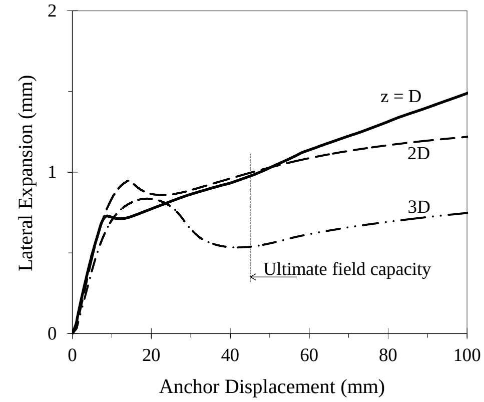

(a) GA3 (L/D = 2.5).

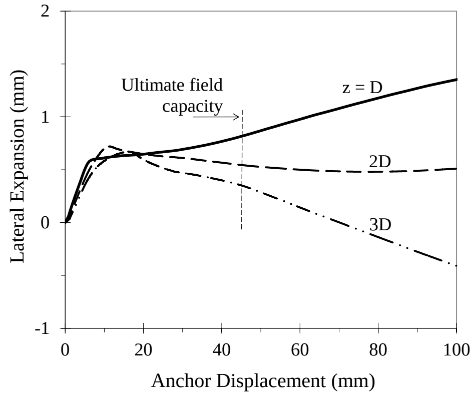

(b) GA7 (L/D = 3.0).

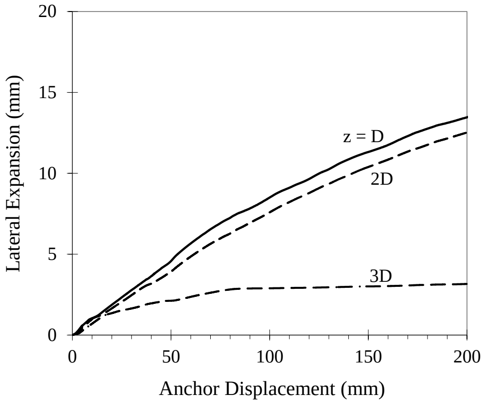

(c) GA2 (L/D = 4.4).

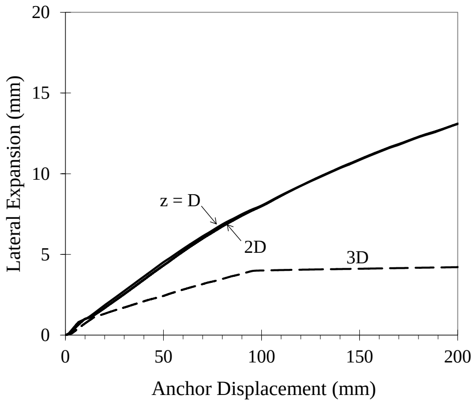

(d) GA4 (L/D = 4.6).

Figure 10(a–d). Predicted radial expansion of gravel column for different z/D_o ; where z is the distance from the column base. Unless otherwise stated, simulations are for a constant ψ' = 10°.

Figure 10(e–h) continued on next page

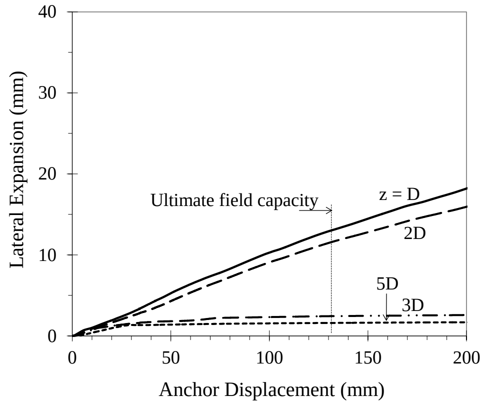

(e) GA6 (L/D = 4.8).

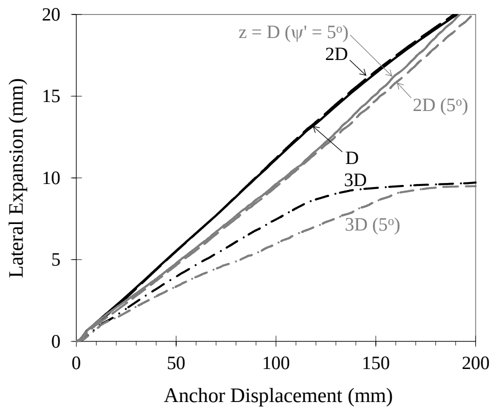

(f) GA1 (L/D = 5.5).

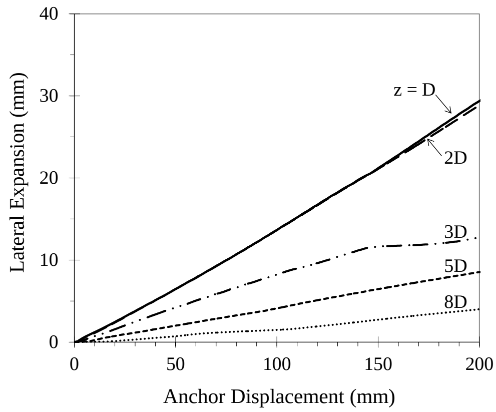

(g) GA5 (L/D = 8.7).

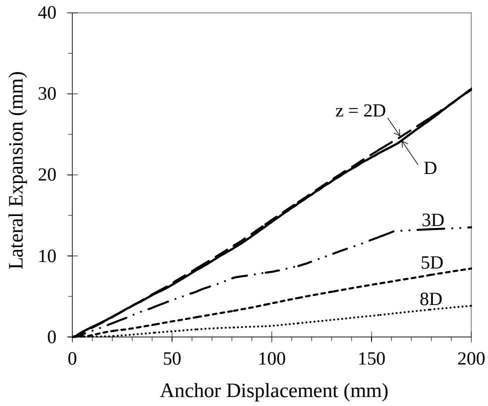

(h) GA8 (L/D = 9.6).

Figure 10(e–h). Predicted radial expansion of gravel column for different z/D_o; where z is the distance from the column base. Unless otherwise stated, simulations are for a constant ψ' = 10^{o}.

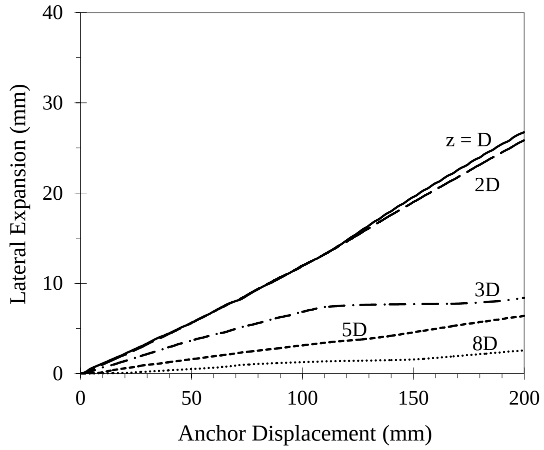

(a) GA5 (L/D = 8.6).

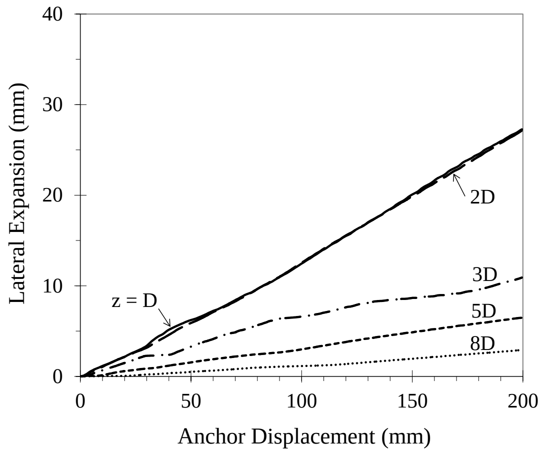

(b) GA8 (L/D = 9.6).

Figure 11. Predicted radial expansion of gravel column for a constant ψ' = 5^{o}.

O'Kelly B.C., Brinkgreve R.B.J. and Sivakumar V. (2014) Pullout resistance of granular anchors in clay for undrained condition. *Soils and Foundations* Vol. 54, No. 6, pp. 1145–1158.

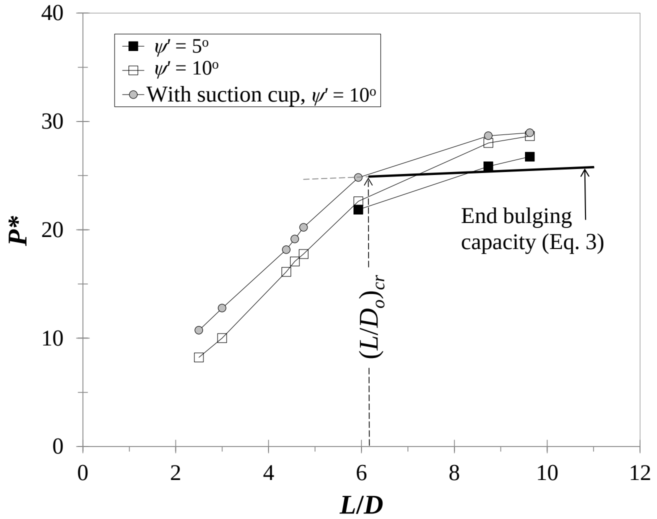

Figure 12. P^* predictions against column L/D ratio.

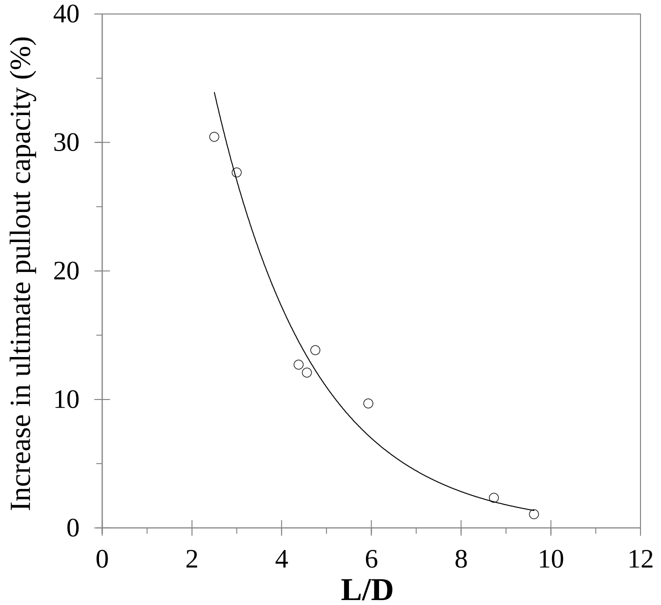

Figure 13. Predicted increase in ultimate pullout capacity for suction of one atmosphere developed beneath the anchor base plate (assuming constant $\psi' = 10^{o}$ for gravel column).

<u>END</u>